



## Heat Transfer in Microchannel Heat Sink Using Nanofluids

N. A. Hamshary and A. R. Shmouty\*

*Mechatronics Department, Faculty of Engineering, Delta University for Science and Technology*

\* Corresponding author at: Mechatronics Department, Faculty of Engineering, Delta University for Science and Technology, Gamasa, Egypt., Tel.: +201223319556; e-mail address: [dr.ahmed@deltauniv.edu.eg](mailto:dr.ahmed@deltauniv.edu.eg).

### ABSTRACT

Convective heat transfer using nanofluid in microchannel heat sink has been performed numerically. Rectangular, semi-circular, triangular and trapezoidal cross section shapes of microchannel heat sink are employed in this present study. ANSYS Workbench 15.0 is set up to solve three-dimensional laminar flow of fluid and heat transfer in microchannel heat sink using the fluid flow system in ANSYS FLUENT. The working fluid used is Al<sub>2</sub>O<sub>3</sub>/water nanofluid with nanoparticle concentrations in the range of (0%-5%). All microchannel heat sink walls are set as adiabatic walls, while the heated plate is set at constant temperature of 340K. Uniform velocity and 300K constant temperature are considered at inlet. Effect of the four cross-sectional shapes on the behavior of heat transfer and Darcy friction factor is studied at Reynolds number is in the range (100-900). Average and local Nusselt number and Darcy friction factor are calculated. The effect of nanofluid concentration on Nusselt number, Darcy friction factor and thermal-hydraulic behavior is studied. Similarity between the results found in the present study and results found in literature is apparent.

**Keywords:** Laminar flow, microchannel heat sink, nanofluid, ANSYS FLUENT.

### 1. Nomenclature

CFD	Computational fluid dynamic		<b>Greek symbols</b>		
$C_p$	Specific heat at constant pressure	J.kg <sup>-1</sup> .K <sup>-1</sup>	$\alpha$	Thermal diffusivity $k/\rho C_p$	m <sup>2</sup> .s <sup>-1</sup>
$D_h$	Hydraulic diameter	$\mu\text{m}$	$\eta$	Thermal hydraulic performance	
$h$	Convective heat transfer coefficient	W.m <sup>-2</sup> .K <sup>-1</sup>	$\mu$	Dynamic viscosity	kg.m <sup>-1</sup> .s <sup>-1</sup>
$f$	Darcy friction factor		$\rho$	Density	kg.m <sup>-3</sup>
$k$	Fluid thermal conductivity	W.m <sup>-1</sup> .K <sup>-1</sup>	$\varphi$	Particle volume fraction	
$Nu$	Nusselt number ( $h_{av}D_h/k$ )		$\tau$	Shear stress	kg.m <sup>-2</sup>
$p$	Pressure	Pa	<b>Subscripts</b>		
$q''$	Heat flux	W.m <sup>-2</sup>	$av$	Average	
$Re$	Reynolds number ( $\rho u D_h/\mu$ )		$b$	Bulk	
$T$	Thermodynamic temperature	K	$bf$	Base fluid	
$u$	Velocity component in $x$ direction	m.s <sup>-1</sup>	$in$	Inlet	
$v$	Velocity component in $y$ direction	m.s <sup>-1</sup>	$nf$	Nanofluid	
$w$	Velocity component in $z$ direction	m.s <sup>-1</sup>	$np$	Nanoparticle	
$x, y, z$	Cartesian coordinate		$out$	Outlet	

### 2. Introduction

Microchannel heat exchanger contributes significantly in heat dissipation from electronic components with high heat generation. Nanofluids becomes the most optimal coolant for electronic components to improve their efficiency promotion and stable operation. Study of heat transfer and fluid flow in microchannels drew more attention due to their wide use in both engineering and medical fields such as CPUs, macro-scale and micro-scale heat exchangers, internal cooling of gas turbines, fuel elements in nuclear power stations and biomedical applications. Considering two types of nanofluids, copper-oxide nanospheres at low volume fractions in water or ethylene glycol, (J. Koo *et al*) solved numerically the conjugated heat transfer problem for micro heat sinks. (J. Lee *et al*) made an experiment to study the benefits of low concentrated Al<sub>2</sub>O<sub>3</sub>/water nanofluids in microchannel cooling

and showed that high thermal conductivity of nano-particles enhanced single phase heat transfer coefficient specially in laminar flow. (Xi Lu *et al*) used manifolds of trapezoid shape to guarantee a uniformly distributed flow in the microchannels and showed that uniform flow in the microchannels depended greatly on the cross-section of the manifold, position and length of inlets and outlets, and the flow rate at inlets. (H. Shokouhmand *et al*), analyzed silicon-based microchannel heat-sinks with a mix of nano-scale Copper particle and pure water in different volume concentrations as a nanofluid coolant. the flow in laminar and turbulent systems with the theoretical and experimental equations was examined using a computer neural-network to replicate laminar flow in micro-channel heat sinks. (H. Mohammed *et al*) examined numerically how the use of nano-fluids affects heat transfer and fluid flow properties in rectangle cross-sectional micro-channel heat sinks using Reynolds number between 100 and 1000. The micro-channel heat sink behavior was examined using  $\text{Al}_2\text{O}_3$ /water nanofluid with volume concentrations between 1% and 5%. (S. Hosseini *et al*) treated numerically the laminar flow of ethylene-glycol nanofluid containing 4% volume concentration of copper oxide using a silicon rectangle shaped micro-channel heat sinks with fixed hydraulic radius and changing width to height ratios, and a constant heat flux. The effect of varying the width to height ratios on pressure loss, coefficient of heat transfer, Nusselt number, and nondimensional temperature in fluid state and solid state was examined with the finite-volume method. (R. Gautam *et al*) comparatively analyzed the behavior of different shapes of micro-channel heat sink for copper-oxide/water nanofluids compared to pure water flow. Nusselt and Poiseuille numbers were studied for each micro-channel and thermophysical characteristics of copper-oxide/water nanofluid. (T. Teng *et al*) used an aluminum  $\text{Al}_2\text{O}_3$ /water nanofluid to test the viability of using it in cooling of electronic chips with a heat exchanger cooled by air. Three different fractions of the nanofluid (0.5, 1.0, and 1.5 wt. %) were synthesized and used in the experiment. The result of the experiment revealed that the heat exchange capacity of nanofluids was greater than water, and a higher volume fractions of nano particles resulted in improved ratios of heat exchange. (W. Escher *et al*) presented an analysis of the characteristics of silica/water nanofluid with volume fractions up to 31%. The thermophysical characteristics of the fluid were measured experimentally. Micro-channel heat sink was made with three widths and their thermal behavior characteristics were described as a function of the volume flow rate for the silica/water nanofluid at volume fractions of 0%, 5%, 16%, and 31%. (W. Duangthongsuka *et al*) presented an experiment to study the heat transfer and pressure loss properties of  $\text{Al}_2\text{O}_3/\text{H}_2\text{O}$  nanofluid through micro-channel heat sinks. The effect of Reynolds number and particles volume fraction on heat transfer and flow had been studied and revealed that the extent of heat transfer of micro-channel heat sinks improved by increasing Reynolds number and particles volume fraction. (M. Kalteh *et al*) compared between an experimental study on a silicon-based chip having glass layered micro-channels, and a numerical study of the two phase Eulerian approach by the use of the finite-volume method, and showed that two phase results were are more similar to results from experiment than single phase models. (A. Albdoor) investigated numerically how the use of nanofluids affect heat transfer and aerodynamics properties in micro-channel heat sinks of rectangle shape for Reynolds numbers between 100 and 400 and varying values of heat flux (50, 100, 150  $\text{W}/\text{cm}^2$ ) with two types of nanofluid ( $\text{Al}_2\text{O}_3$ /water, Cu/water) with volume fraction 10%. Results revealed that heat transfer as well as pressure loss increase by raising Reynolds number, and the friction coefficient of the micro-channel heat sinks decreases. (A. Sivakumar *et al*) studied experimentally and numerically heat transfer properties of serpentine shape micro-channel heat sinks with  $\text{Al}_2\text{O}_3/\text{H}_2\text{O}$  nanofluids and suggested that the greatest heat transfer improvement could be accomplished by the use of serpentine shaped micro-channel with an  $\text{Al}_2\text{O}_3/\text{H}_2\text{O}$  nanofluid as coolant. (H. Patel *et al*) analyzed heat transfer in silicon micro channel heat sink using  $\text{Al}_2\text{O}_3$ /water mixes with no scattering as coolant. The  $\text{Al}_2\text{O}_3$  particles volume concentration was 5% and showed that micro-channel heat sinks with nanofluids as coolant can take in more heat than micro-channel heat sinks with water as coolant. (S. Barad *et al*) studied the performance of micro-channel heat sinks with rectangle shape with  $\text{Al}_2\text{O}_3/\text{H}_2\text{O}$  as a base nanofluid and showed that thermal conductance of nano particles enhanced the single-phase coefficient of heat transfer for laminar flows. (Y. Yue *et al*) studied fluid and thermal behavior of manifolds microchannel heat sinks using nanofluids and pure water using finite volume method, showing that by raising volume concentration of nano-particles, Nusselt number as well as pumping power increased, but total entropy generation decreased. (L. Chai *et al*) studied numerically laminar flow in micro-channel heat sink having triangle ribs on walls and the effect of triangle ribs shape and distribution on local fluid flow and heat transfer properties, showing that, using mounted triangle ribs on the parallel walls of micro-channels causes a significant improvement on heat transfer, but is accompanied with a great pressure loss. Accordingly, and throughout above researches, enhancement of heat transfer in micro-channel heat sink still need more research. The aim of the present work is to study laminar flow and heat transfer characteristics on microchannel heat sinks of four cross section shapes (rectangular - semicircular - triangular - trapezoidal) using  $\text{Al}_2\text{O}_3$ /water nanofluid with six concentrations ranged from 0% (pure water) to 5%, and Reynolds number between 100 and 900, to illustrate the effects of cross section shaped, nanofluid volume fraction, and Reynolds number, on the performance of microchannel heat sink.

**3. Mathematical Modeling**

Figure (1) describes the developed three-dimensional model. The geometrical model consists of a rectangular heated plate covered with microchannel heat sink. The generated heat at heated plate of thickness  $t$  ( $\mu m$ ) and depth  $l$  ( $\mu m$ ) is removed by flowing fluid through the microchannel heat sink aluminum strips.

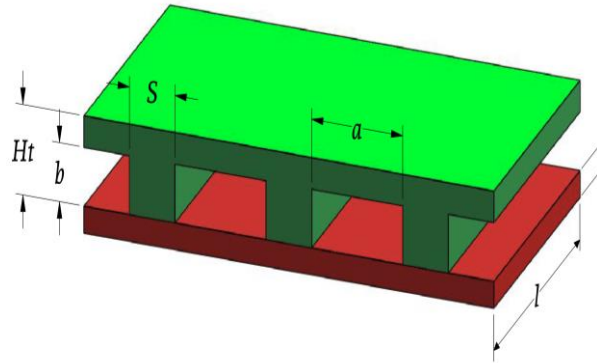


**Fig. (1)** Microchannel heat sink description

The microchannel heat sink consists of multi channels aluminum strips with cross section dimensions listed in table (1) and showed in figure (2) as follow:

**Table (1)** Dimensions of microchannel heat sink cross sections

	Rectangular	Semi-circular	Tri-angular	Trapezoidal	
$a$	200	---	200	200	$\mu m$
$b$	88	---	---	100	$\mu m$
$H$	---	---	195	110.5	$\mu m$
$R$	---	100	---	---	$\mu m$
$Dh$	122.2	122.2	122.2	122.2	$\mu m$
$l$	1000	1000	1000	1000	$\mu m$
$S$	100	100	100	100	$\mu m$
$Ht$	135	150	245	160.5	$\mu m$
$t$	50	50	50	50	$\mu m$

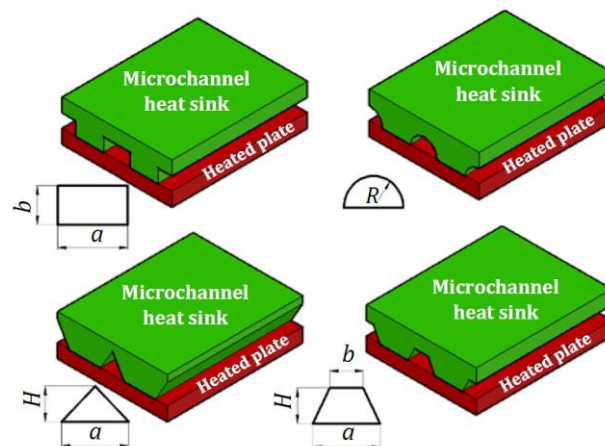


**Fig. (2)** Geometry of microchannel heat sink cross sections

The flow is considered steady and laminar with constant thermo-physical properties. Nanofluid is considered to be incompressible. The effects of radiative transport and viscous dissipation are assumed to be neglected. Uniform heated plate walls temperature boundary conditions are set as 340K while all microchannel

heat sink surfaces are assumed as adiabatic surfaces. Nano-fluid flow has uniform velocity and uniform temperature of 300K at the inlet of the microchannel heat sink.

Fluid flow and heat transfer in a microchannel heat sink can be modelled using three-dimensional governing conservations summarized as conservation of mass, conservation of energy and conservation of momentum.

Cartesian coordinate system is used to describe the fluid flow. Based on the assumptions that simplify the equations, the main equations in three dimensions that govern the flow are summarized as follows:

Conservation of mass:

$$\frac{\partial u}{\partial x} + \frac{\partial v}{\partial y} + \frac{\partial w}{\partial z} = 0 \quad (1)$$

Conservation of momentum:

$$\rho \left( u \frac{\partial u}{\partial x} + v \frac{\partial u}{\partial y} + w \frac{\partial u}{\partial z} \right) = -\frac{\partial p}{\partial x} + \mu \left( \frac{\partial^2 u}{\partial x^2} + \frac{\partial^2 u}{\partial y^2} + \frac{\partial^2 u}{\partial z^2} \right) \quad (2)$$

$$\rho \left( u \frac{\partial v}{\partial x} + v \frac{\partial v}{\partial y} + w \frac{\partial v}{\partial z} \right) = -\frac{\partial p}{\partial y} + \mu \left( \frac{\partial^2 v}{\partial x^2} + \frac{\partial^2 v}{\partial y^2} + \frac{\partial^2 v}{\partial z^2} \right) \quad (3)$$

$$\rho \left( u \frac{\partial w}{\partial x} + v \frac{\partial w}{\partial y} + w \frac{\partial w}{\partial z} \right) = -\frac{\partial p}{\partial z} + \mu \left( \frac{\partial^2 w}{\partial x^2} + \frac{\partial^2 w}{\partial y^2} + \frac{\partial^2 w}{\partial z^2} \right) \quad (4)$$

Conservation of energy:

$$u \frac{\partial T}{\partial x} + v \frac{\partial T}{\partial y} + w \frac{\partial T}{\partial z} = \alpha \left( \frac{\partial^2 T}{\partial x^2} + \frac{\partial^2 T}{\partial y^2} + \frac{\partial^2 T}{\partial z^2} \right) \quad (5)$$

Where  $u$ ,  $v$  and  $w$  are the velocities in  $x$ ,  $y$  and  $z$  direction, respectively. In addition,  $p$ ,  $\rho$ ,  $\mu$  and  $\alpha$  are the fluid pressure, density, dynamic viscosity, and thermal diffusivity, respectively. Equations (1) through (5) are used in the computational system of the model. The overall performance of presented laminar forced convection in the three-dimensional microchannel heat sink is evaluated through average Nusselt number and average Darcy friction factor. Reynolds number can be defined as:

$$Re = \frac{\rho u D_h}{\mu} \quad (6)$$

Where  $D_h$  (m) is the hydraulic diameter, which can be calculated for every cross section as follow:

For rectangular cross section,

$$D_h = \frac{2(a \times b)}{(a+b)} \quad (7)$$

For semi-circular cross section,

$$D_h = \frac{2\pi R}{(\pi+2)} \quad (8)$$

For triangular cross section,

$$D_h = \frac{2(a \times H)}{\left( a + 2\sqrt{\left(\frac{a}{2}\right)^2 + H^2} \right)} \quad (9)$$

For trapezoidal cross section,

$$D_h = \frac{2H(a+b)}{\left( a+b+2\sqrt{\left(\frac{a-b}{2}\right)^2 + H^2} \right)} \quad (10)$$

The average Darcy friction factor can be used to represent the flow characteristics as:

$$f = \frac{2\bar{\tau}_w}{\rho u^2} \quad (11)$$

Where,  $f$  is the average Darcy friction factor and  $\bar{\tau}_w$  is the average wall shear stress at heated plate. Local wall shear stress can be calculated as:

$$\tau = \mu \left( \frac{\partial u}{\partial y} \right) \quad (12)$$

Average wall shear stress at heated plate:

$$\bar{\tau}_w = \frac{\int_0^L \tau dz}{\int_0^L dz} \quad (13)$$

Local Nusselt number at heated plate can be calculated as:

$$Nu = \frac{q'' D_h}{k(T_w - T_b)} \quad (14)$$

Where  $q''$  is the local heat flux at heated plate,  $T_w$  and  $T_b$  are wall and bulk temperatures respectively.

Local heat flux is introduced as:

$$q'' = -k \left( \frac{\partial T}{\partial y} \right) \quad (15)$$

Average heat flux is:

$$\overline{q_w} = \frac{\int_0^L q'' dz}{\int_0^L dz} \quad (16)$$

Average Nusselt number at heated plate can be calculated as:

$$Nu_{av} = \frac{h_{av} D_h}{k} = \frac{D_h \overline{q_w}}{k(T_w - T_{b,av})} \quad (17)$$

Where  $h_{av}$  is the average coefficient of heat transfer,  $k$  is the nanofluid thermal conductivity and  $T_{b,av}$  is the flow average bulk temperature that can be calculated as:

$$T_{b,av} = \frac{T_{b,in} + T_{b,out}}{2} \quad (18)$$

Where  $T_{b,in}$  and  $T_{b,out}$  are inlet and outlet bulk temperatures respectively. The thermo-physical characteristics for the nano-particle ( $Al_2O_3$ ), base fluid (water), and the  $Al_2O_3$ /water nanofluid of six different concentration are listed in Table 2.

**Table (2)** Thermo-physical properties of  $Al_2O_3$ , water and nanofluid at 300K

	$\rho$ (kg/m <sup>3</sup> )	$C_p$ (J/kg.K)	$K$ (W/m.K)	$\mu$ (kg/m.s)
( $Al_2O_3$ )	3970	765	40	---
Pure water; $\varphi=0\%$	998.2	4182	0.613	0.001003
<i>nf</i> ; $\varphi=1\%$	1027.918	4050.029	0.630739	0.001028
<i>nf</i> ; $\varphi=2\%$	1057.636	3925.475	0.648824	0.001053
<i>nf</i> ; $\varphi=3\%$	1087.354	3807.729	0.667264	0.001078
<i>nf</i> ; $\varphi=4\%$	1117.072	3696.248	0.686071	0.001103
<i>nf</i> ; $\varphi=5\%$	1146.79	3590.545	0.705255	0.001128

Thermo-physical properties of nanofluid:

Density:

$$\rho_{nf} = (1 - \varphi)\rho_{bf} + \varphi\rho_{np} \quad (19)$$

Specific heat:

$$C_{p,nf} = \frac{(1-\varphi)(\rho C_p)_{bf} + \varphi(\rho C_p)_{np}}{\rho_{nf}} \quad (20)$$

Thermal conductivity:

$$k_{nf} = \frac{k_{np} + 2k_{bf} + 2\varphi(k_{np} - k_{bf})}{k_{np} + 2k_{bf} - \varphi(k_{np} - k_{bf})} k_{bf} \quad (21)$$

Viscosity:

$$\mu_{nf} = \mu_{bf}(1 + 2.5\varphi) \quad (22)$$

Where  $\varphi$  is the volume concentration of particles, nanofluid properties have subscript '*nf*', base fluid properties have subscript '*bf*', and particle properties have subscript '*np*'.

The thermal hydraulic performance is calculated as :

$$\eta = \frac{Nu_{nf}}{Nu_{water}} \left( \frac{f_{nf}}{f_{water}} \right)^{1/3} \quad (23)$$

#### 4. Numerical Solution

ANSYS Workbench 15.0 is configured to find a solution to three-dimensional laminar fluid flow and heat transfer in microchannel heat sink using the fluid flow system ANSYS FLUENT. The model geometry and the corresponding computational mesh are presented using the geometry and meshing tools within design modeler and meshing tools in ANSYS Workbench. ANSYS FLUENT Launcher is used to configure and solve the present computational fluid dynamic CFD problem, then view the result in both ANSYS FLUENT and the ANSYS CFD postprocessing tool. The computational domain is depicted as in Figure (1). The finite volume method is used in ANSYS FLUENT Workbench as a base for the computational scheme. In the presented study, non-uniform grids and the cells near the walls have fine mesh. A high-density grid is used at the heat transfer wall while a uniformly distributed grid is used in the flow direction as shown in Figure (3).

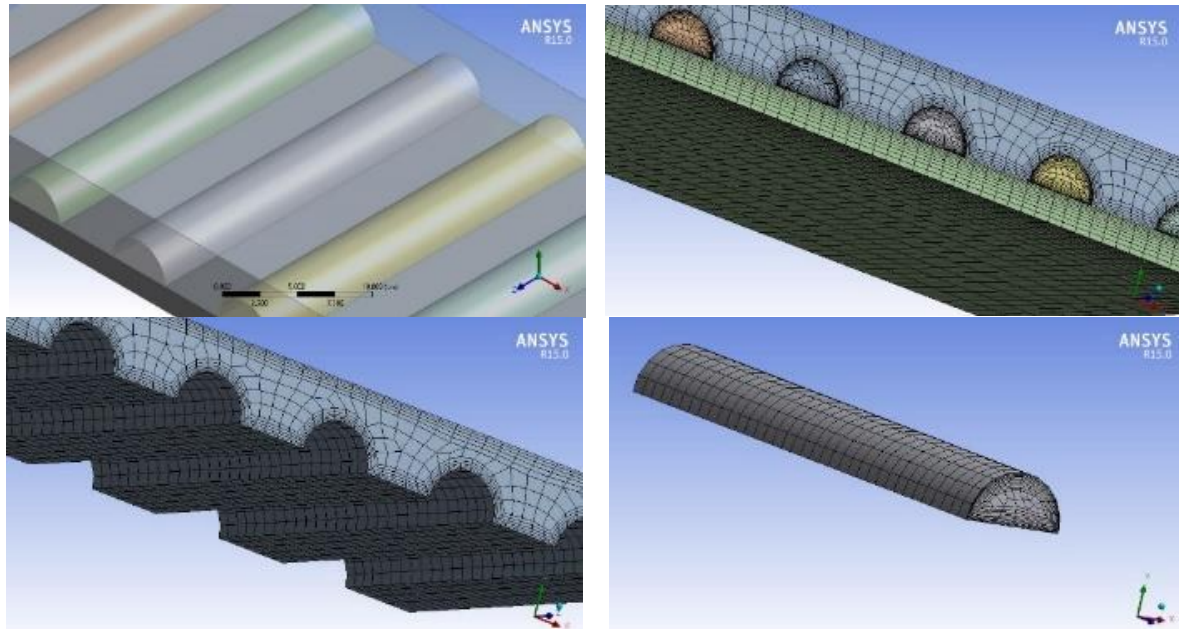


**Fig. (3)** The Generated mesh

It was found that, the results accuracy is affected by the number and the size of the cells for the generated mesh. Using a grid independence study, cell sizes are changed inside the computational model and the obtained results are used to choose grid sizes. Multiple meshes are used in testing to ensure that the solution is not affected by mesh size. Figure (4) illustrates the change of average Nusselt number and average Darcy friction factor with the number of cells at generated mesh. Grid dependency test indicates that 25000 cells with 27846 nodes is suitable. It is shown that, refining the grids further had negligible changes in the result for average Nusselt number and average Darcy friction factor.

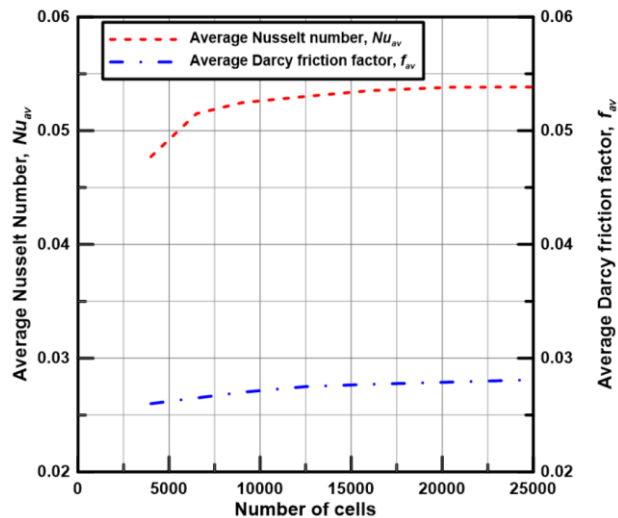


**Fig. (4)** Grid independence study

A double precision 3D ANSYS FLUENT Launcher and laminar viscous flow are adjusted for created nanofluid as a working fluid. The standard SIMPLE algorithm is employed for pressure velocity coupling. The second-order upwind method is selected for both momentum and energy terms. Pressure and momentum relaxation factor in ANSYS FLUENT are varied to reach convergence. Obtained results reaches convergence when residual values are less than or equal to the selected values which are set as  $10^{-4}$  for continuity while velocity components and energy residual is set as  $10^{-7}$  as shown in figure (5).

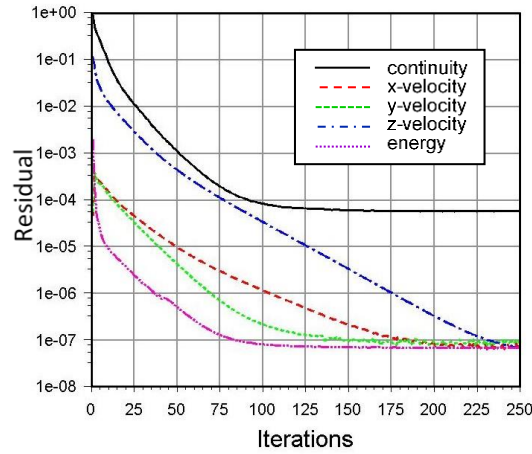


Fig. (5) Numerical model iteration

## 5. Results and Discussions

Laminar forced convection heat transfer in microchannel heat sink with varying cross section shape using nanofluid is studied numerically. To verify how accurate the numerical model is, a comparison is made between the result of the present work with the results reached by (Lee *et al*) and (Mohammed *et al*). Figure (6) shows the variation of average Darcy friction factor with Reynolds number  $Re$  for rectangular microchannel heat sink using nanofluid with concentration  $\phi = 1\%$ . Present work shows high similarity with both results of (Lee *et al*) and (Mohammed *et al*).

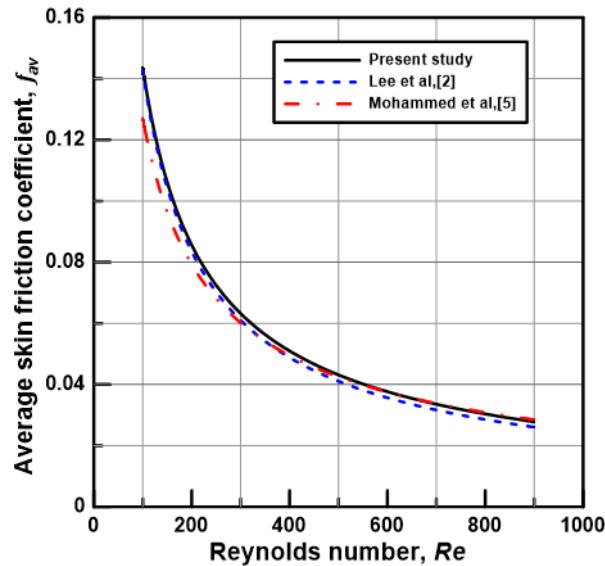
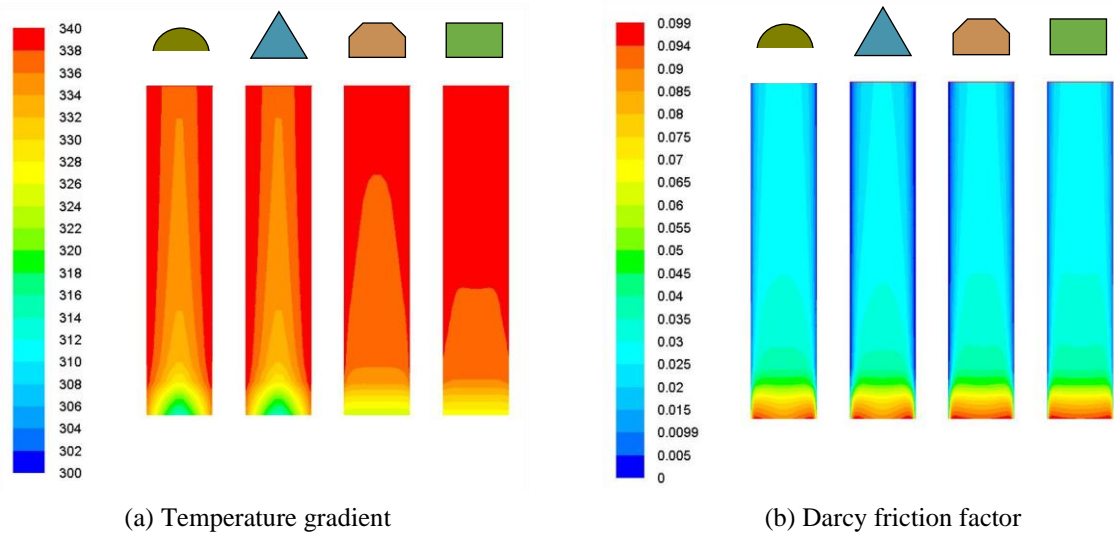


Fig. (6) Comparison between Average Darcy friction factor for different Reynolds numbers with reported results

Figure (7) indicates the influence of microchannel cross section shape on fluid behavior. Water is used as the working fluid with  $Re = 900$  and  $300K$  at inlet. It is observed that, circular cross section shape has the greatest effect on temperature gradient along the heated plate more than other cross section shapes while rectangular cross section shape has the lowest effect as shown in figure (7-a). While, figure (7-b) indicates that, triangular cross section shape has a significant effect on Darcy friction factor distributions near microchannel sidewalls more than other cross section shapes. These observations do not give an accurate assessment for the effect of cross section shape on heat transfer improvement in micro-channel heat sinks. Therefore, average Nusselt number and Darcy friction factor along the heated plate are essential in studying the effect of cross section shape and nanofluid concentrations on heat transfer enhancement in micro-channel heat sink.



**Fig. (7)** Effect of microchannel cross section shape on temperature and Darcy friction factor distribution

**5.1 Effect of cross section shape on Darcy friction factor**

Figure (8) illustrate average Darcy friction factor at different Reynolds numbers for four microchannel cross-section shapes. Water is used as the working fluid with inlet temperature 300K and Reynolds number is ranged from (100 – 900). As shown in figure (8), average Darcy friction factor at the heated plate decreases with increasing Reynolds number for all cross-section shapes. Moreover, microchannel heat sinks with rectangle cross-section shape has the highest average Darcy friction factor while triangular cross section shape has the lowest average Darcy friction factor.

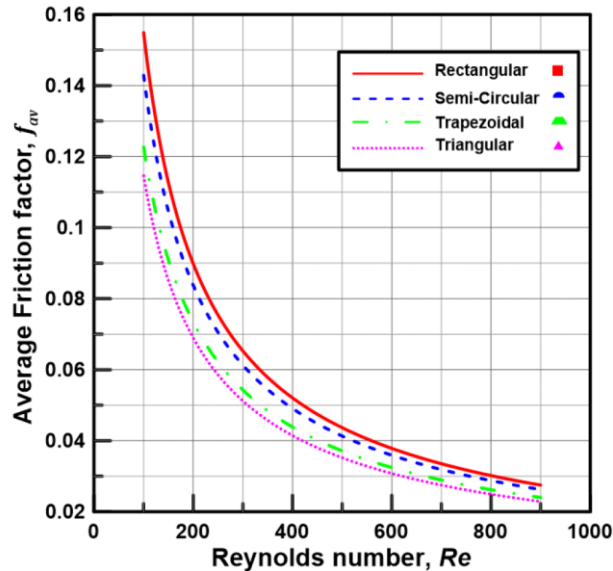


**Fig. (8)** Average Darcy friction factor at heated plate

**5.2 Effect of cross section shape on Nusselt number**

Figure (9) shows the change of average Nusselt number with respect to Reynolds number for four microchannel cross-section shapes. Water is used as the working fluid with inlet temperature 300K and Reynolds number is ranged from (100 – 900).



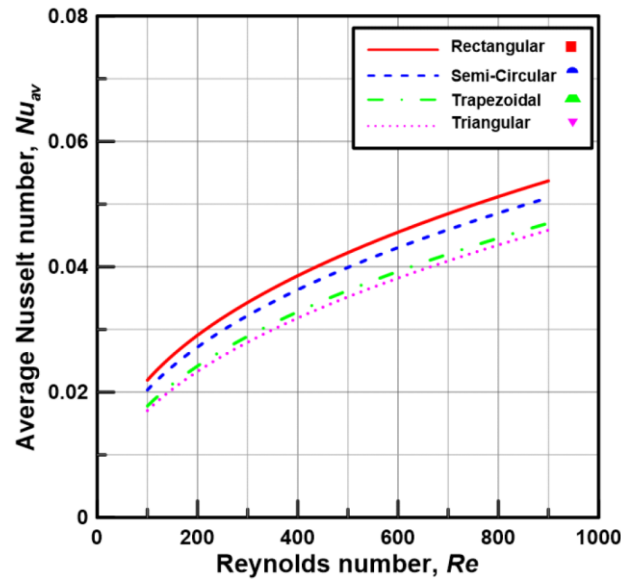


Fig. (9) Average Nusselt number at heated plate

As shown in figure (9), average Nusselt number at the heated plate rises with raising Reynolds number for all cross-section shapes. In addition, microchannel heat sink with rectangle cross-section shape has the highest average Nusselt number while triangular cross section shape has the lowest average Nusselt number. It is clear from figures (8) and (9) that, rectangular cross section shape is more suitable in improving heat transfer in micro-channel heat sink.

### 5.3 Effect of nanofluid concentration on Darcy friction factor

$Al_2O_3$ /water nanofluid with six concentrations in the range of  $\phi = 0\%$  (pure water),  $\phi = 1\%$ ,  $\phi = 2\%$ ,  $\phi = 3\%$ ,  $\phi = 4\%$  and  $\phi = 5\%$ , is used as the working fluid with inlet temperature 300K and  $Re=100$ . Rectangular cross section microchannel heat sink is studied. Figure (10) represents local Darcy friction factor at the axis of symmetry along the heated plate. It is clear that, local Darcy friction factor increases with increasing nanoparticle concentrations of nanofluid. Pure water with nanoparticle concentration  $\phi = 0\%$  has the lowest local Darcy friction factor, while nanofluid with nanoparticle concentration  $\phi = 5\%$  has the highest local Darcy friction factor.

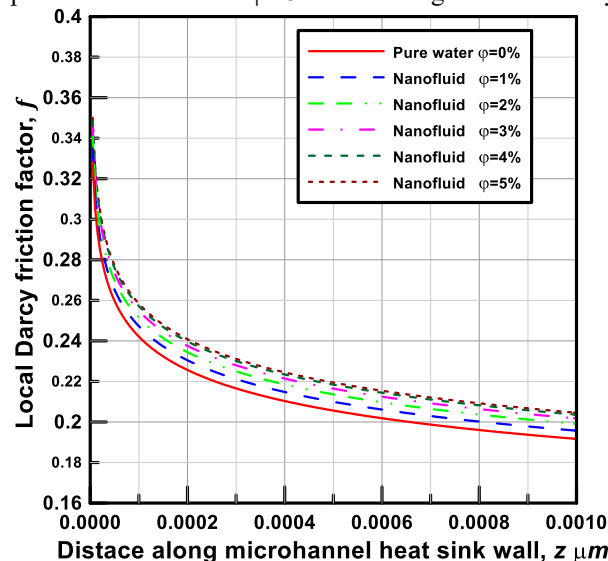
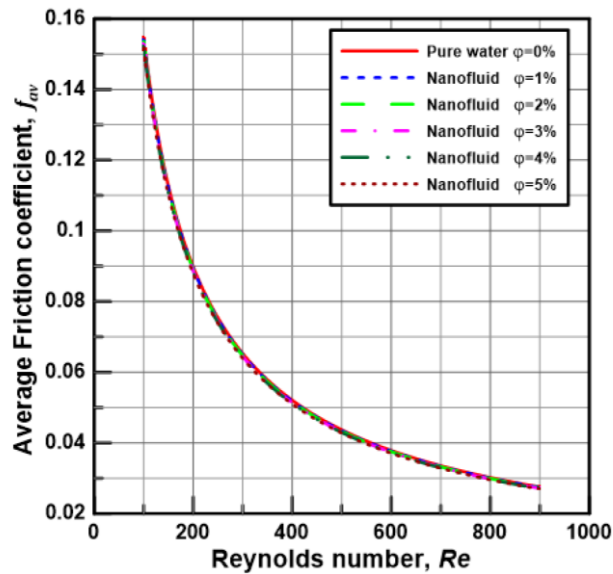


Fig. (10) Local Darcy friction factor at the heated plate for different nanofluid concentrations

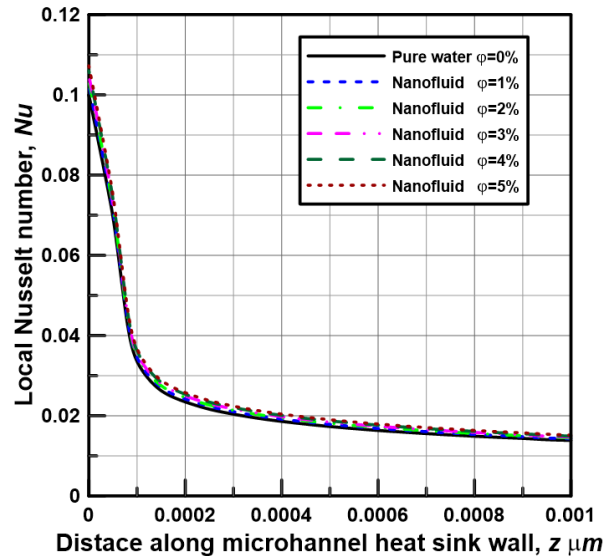
While, changing of fluid nanoparticle concentrations from 0% (pure water) to 5% has slight effect on average Darcy friction factor. as shown in figure (11).



**Fig. (11)** Average Darcy friction factor at the heated plate for different nanofluid concentrations

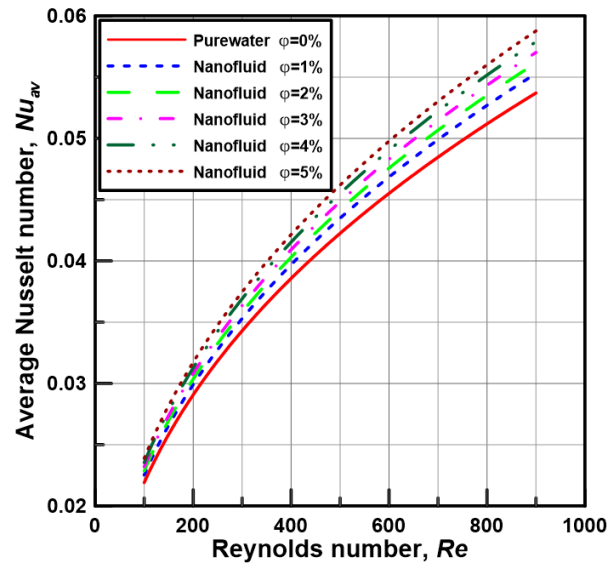
#### 5.4 Effect of nanofluid concentration on Nusselt number

Figure (12) illustrates the change of local Nusselt number at the axis of symmetry along the heated plate. Nanofluid with nanoparticle concentrations are in the range of ( $\phi = 0\% - 5\%$ ) is used with inlet temperature 300K and  $Re=100$ . Rectangular cross section microchannel heat sink is studied.



**Fig. (12)** Local Nusselt number at the heated plate for different nanofluid concentrations

As shown in figure (12), local Nusselt number increases with increasing nanoparticle concentrations of nanofluid. Nanofluid with nanoparticle concentration  $\phi = 5\%$  has the highest local Nusselt number while pure water with nanoparticle concentration  $\phi = 0\%$  has the lowest local Nusselt number. In the same manner, figure (13) shows that, average Nusselt number increases with increasing nanoparticle concentrations of nanofluid. Nanofluid with nanoparticle concentration  $\phi = 5\%$  has the highest average Darcy friction factor, while pure water with nanoparticle concentration  $\phi = 0\%$  has the lowest average Nusselt number. Also, effect of nanoparticle concentration on average Nusselt number increases with increasing Reynolds number.



**Fig. (13)** Average Nusselt number at the heated plate for different nanofluid concentrations

### 5.5 Effect of nanofluid concentration on the thermal hydraulic performance

Figure (14) shows the effect of nanofluid concentration on the thermal hydraulic performance at  $Re=300$ . It is found that, thermal hydraulic performance increases with increasing nanofluid concentration. In addition, microchannel heat sink with rectangular and semi-circular cross section shapes have the highest thermal hydraulic performance while trapezoidal and triangular cross section shape have the lowest thermal hydraulic performance.

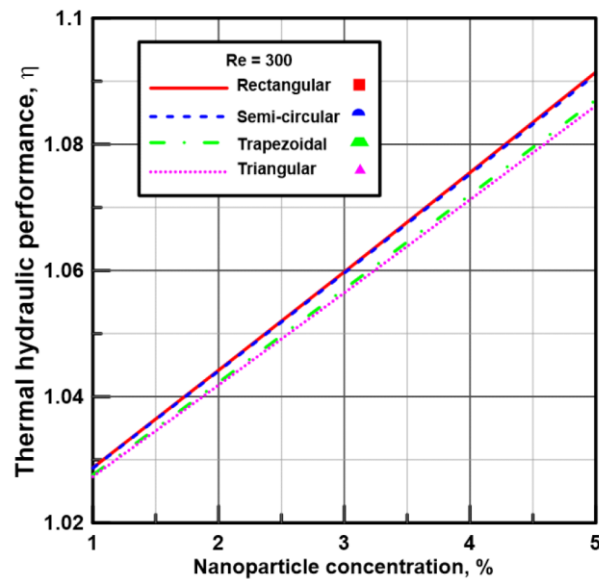


**Fig. (14)** Thermal hydraulic performance for different microchannel heat sink cross sections

### 5.6 Effect of Reynolds number on the thermal hydraulic performance

Figure (15) shows the effect of Reynolds number on the thermal hydraulic performance for nanofluid concentration  $\phi=3\%$ . It is found that, thermal hydraulic performance increases with increasing Reynolds number.

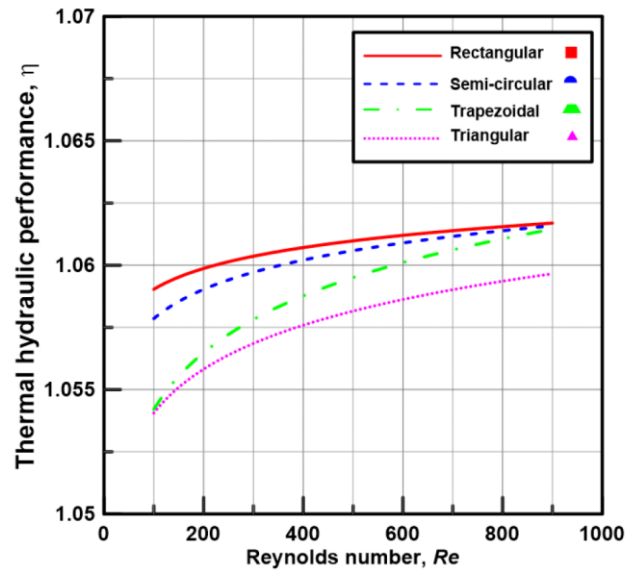


Fig. (15) Thermal hydraulic performance at different Reynolds number

In the same manner, high thermal hydraulic performance is found at microchannel heat sink with rectangular cross section shape while triangular cross section shape has lower thermal hydraulic performance. Also, at high Reynolds number triangular cross section shape has lowest thermal hydraulic performance while the rest three cross sections tend to have the same thermal hydraulic performance.

#### 4. Conclusion

Effect of microchannel heat sink cross section shape and nanofluid concentration on Nusselt number, Darcy friction factor and thermal hydraulic performance for Reynolds number ranges from 100 to 900 are studied. Results shows that, rectangular cross section shape is the more suitable shape in enhancing heat transfer in microchannel heat sink. In addition, with increasing nanofluid concentration, local and average Nusselt number, local Darcy friction factor and in turn thermal hydraulic performance are increased. The nanofluid of concentration  $\phi=5\%$ , has a relative increase of 9.5% in average Nusselt number compared with pure water, while nanoparticle concentrations have slight effect on average Darcy friction factor. Similarity between introduced results in the present study and results found in literature is apparent.

#### Disclosure

This research did not receive any specific grant from funding agencies in the public, commercial or not-for-profit sectors. There is no Conflict of Interest

#### References

- A. Sivakumar, N. Alagumurthi and T.Senthilvelan, Heat transfer enhancement of serpentine shaped micro channel heat sink with AL<sub>2</sub>O<sub>3</sub>/water nanofluid, International Journal of Technical Research and Applications, 2 Issue 4 112-116, (2014).
- Ahmed Khafeef Obaid Albdoor, Numerical investigation of laminar nanofluid flow in micro channel heat sinks, International Journal of Mechanical Engineering and Technology, 5 Issue 12, 86-96,(2014).
- H.A. Mohammed, P. Gunnasegaran and N.H. Shuaib, Heat transfer in rectangular microchannels heat sink using nanofluids, International Communications in Heat and Mass Transfer, 37, 1496–1503, (2010).
- Harish Kumar Patel, Rupesh Kumar Khutey, Alok Kumar Verma and Sameer Verma, Assessment of the effectiveness of nanofluids for single-phase heat transfer in micro-channels, Asian Resonance,III Issue-IV, 73-77, (2014).
- Hossein Shokouhmand, Mohammad Ghazvini and Jaber Shabaniyan, Performance analysis of Using nanofluids in microchannel heat sink in different flow regimes and its simulation using artificial neural network, Proceedings of the World Congress on Engineering Vol III, WCE 2008, London, U.K, (2008).
- J. Koo and C. Kleinstreuer, Laminar nanofluid flow in microheat-sinks, International Journal of Heat and Mass Transfer, 48, 2652–2661, (2005).
- Jaeseon Lee and Issam Mudawar, Assessment of the effectiveness of nanofluids for single-phase and two-phase

- heat transfer in micro-channels, *International Journal of Heat and Mass Transfer*, 50, 452–463, (2007).
- Lei Chai, Liang Wang and Xin Bai, Thermohydraulic performance of microchannel heat sinks with triangular ribs on sidewalls – Part 1: Local fluid flow and heat transfer characteristics, *International Journal of Heat and Mass Transfer*, 127,1124–1137, (2018).
- Lei Chai, Liang Wang and Xin Bai, Thermohydraulic performance of microchannel heat sinks with triangular ribs on sidewalls – Part 2: Average fluid flow and heat transfer characteristics, *International Journal of Heat and Mass Transfer*, 128,634–648, (2019).
- Mohammad Kalteh , Abbas Abbassi , Majid Saffar-Avval, Arjan Frijns , Anton Darhuber and Jens Harting, Experimental and numerical investigation of nanofluid forced convection inside a wide microchannel heat sink, *Applied Thermal Engineering*, 36, 260-268, (2012).
- Rajesh Gautam , Avdresh K. Sharma and Kapil D. Gupta, Performance analysis of non-circular microchannels flooded with CuO-water nanofluid, 3rd Micro and Nano Flows Conference Thessaloniki, Greece, (2011).
- Sanjay V. Barad and Mukesh N. Makwana, Numerical investigation of single phase fluid flow and heat transfer in rectangular micro channel using nanofluids as a cooling liquid, *Journal of Engineering Research and Applications*, 4 Issue 4, 133-137, (2014).
- Seyed S. Hosseini and Abbas. Abbassi, Numerical investigation of aspect ratio effect on thermal parameters in laminar nanofluid flow in microchannel heat sink, 3rd Micro and Nano Flows Conference Thessaloniki, Greece, (2011).
- Tun-Ping Teng, Yi-Hsuan Hung, Tun-Chien Teng and Jyun-Hong Chen, Performance evaluation on an air-cooled heat exchanger for alumina nanofluid under laminar flow, *Nanoscale Research Letters*(2011).
- W. Escher, T. Brunschweiler, N. Shalkevich, A. Shalkevich, T. Burgi, B. Michel and D. Poulikakos, On the cooling of electronics with nanofluids, *Journal of Heat Transfer*, 133, 051401-1 - 051401-11, (2011).
- Weerapun Duangthongsuka and Somchai Wongwises, Heat transfer enhancement and flow characteristic of Al<sub>2</sub>O<sub>3</sub>/water nanofluids flowing through a microchannel heat sink, *The Second TSME International Conference on Mechanical Engineering*, Krabi, (2011) .
- Xi Lu and A. G. Agwu Nnanna, Experimental study of fluid flow in microchannel, *ASME International Mechanical Engineering Congress and Exposition*, October 31-November 6, IMECE2008-67932, Boston, Massachusetts, USA, (2008).
- Yun Yue, Shahabeddin K. Mohammadian and Yuwen Zhang, Analysis of performances of a manifold microchannel heat sink with nanofluids, *International Journal of Thermal Sciences*, 89, 305-313, (2015).